Soldati, Marco; Laakso, Ilkka

# Effect of electrical conductivity uncertainty in the assessment of the electric fields induced in the brain by exposure to uniform magnetic fields at 50 Hz

*Published in:*
IEEE Access

*DOI:*
10.1109/ACCESS.2020.3043602

Published: 09/12/2020

*Document Version*
Publisher's PDF, also known as Version of record

IEEE Access
Multidisciplinary | Rapid Review | Open Access Journal

Received November 18, 2020, accepted December 5, 2020, date of publication December 9, 2020,
date of current version December 23, 2020.

*Digital Object Identifier 10.1109/ACCESS.2020.3043602*

# Effect of Electrical Conductivity Uncertainty in the Assessment of the Electric Fields Induced in the Brain by Exposure to Uniform Magnetic Fields at 50 Hz

**MARCO SOLDATI[1] AND ILKKA LAAKSO[1,2], (Member, IEEE)**
[1]Department of Electrical Engineering and Automation, Aalto University, 02150 Espoo, Finland
[2]Aalto Neuroimaging Infrastructure, Aalto University, 02150 Espoo, Finland

Corresponding author: Marco Soldati (marco.soldati@aalto.fi)

This work was supported in part by the Academy of Finland under Grant 325326.

**ABSTRACT** International exposure standard/guidelines establish limits for external electromagnetic field strengths. At low frequencies, these maximum allowable exposure levels are derived from the limits defined for internal electric field strengths which have been set to avoid adverse health effects. In the IEEE International Committee on Electromagnetic Safety standard, the relationship between internal and external fields was obtained through homogeneous elliptical models without considering the dielectric properties of tissues. However, the International Commission on Non-Ionizing Radiation Protection guidelines were established using computational dosimetry on realistic anatomical models. In this case, variability in the electrical conductivity of the tissues represents a major source of uncertainty when deriving allowable external field strengths. Here we characterized this uncertainty by studying the effect of different tissue conductivity values on the variability of the peak electric field strengths induced in the brain of twenty-five individuals exposed to uniform magnetic fields at 50 Hz. Results showed that the maximum electric field strengths computed with new estimations of brain tissue conductivities were significantly lower than those obtained with commonly used values in low-frequency dosimetry. The lower strengths were due to the new brain conductivity values being considerably higher than those usually adopted in dosimetry modeling studies. A sensitivity analysis also revealed that variations in the electrical conductivities of the grey and white matter had a major effect on the peak electric field strengths in the brain. Our findings are intended to lessen dosimetric uncertainty in the evaluation of the electric field strengths due to electrical properties of the biological tissues.

**INDEX TERMS** Anatomical head models, dosimetry, electromagnetic field exposure, induced electric field, low frequency, tissue conductivity.

## I. INTRODUCTION

Safety limits have been established by the International Commission on Non-Ionizing Radiation Protection (ICNIRP) [1] and the Institute of Electrical and Electronics Engineers International Committee on Electromagnetic Safety (IEEE ICES) [2], [3] to protect individuals against adverse health effects that might arise from human exposure to low-frequency (LF) electromagnetic fields. The LF range is defined as the interval of frequencies lower than 10 MHz in the ICNIRP guidelines [1], and below 5 MHz in the IEEE standard [2]. In addition, the World Health Organization [4] further divides the LF interval into extremely low-frequency range (ELF, from 0 Hz to 300 Hz), and intermediate frequency range (IF, from 300 Hz to 10 MHz). In this context, the exposure limits are intended to limit the electric field strength induced by LF time varying electromagnetic fields, which can alter the synaptic activity at ELF or excite nerve and muscle cells at IF [1], [2]. To avoid these adverse health effects, both standard/guidelines established exposure limits termed as basic restrictions [1] or dosimetric reference limits [2], [3], which are expressed in terms of induced electric

The associate editor coordinating the review of this manuscript and approving it for publication was Lei Zhao.

field strength. However, direct measurements of the induced electric field in the human body are not feasible. For this reason, the ICNIRP guidelines and IEEE standard introduced easier dosimetric quantities to measure, namely the reference levels [1] or exposure reference levels [3]. Compliance with the (exposure) reference levels should guarantee that the induced electric fields satisfy the basic restrictions/dosimetric reference limits.

In the ICNIRP guidelines [1], the basic restrictions were derived from published data based on thresholds for the induction of magnetic phosphenes and peripheral nerve stimulation [5]. The reference levels were obtained from the basic restrictions through dosimetry modeling by means of a male and female realistic anatomical models [6], [7]. Uncertainty in computational modeling and variability among the population were taken into account by applying a reduction factor of 3 when deriving the reference levels from the basic restrictions. In the IEEE standard [2], [3], reduction factors were instead applied directly to the dosimetric reference limits, which were derived from threshold data of magnetophosphenes [9], [10] and peripheral nerve stimulation using an excitation model [11]. The exposure reference levels were then obtained using homogeneous elliptical models [2], [3].

As the reference levels were obtained from the basic restrictions using anatomical models, one of the most important source of uncertainty is represented by the estimation of the tissue electrical conductivities. A recent ICNIRP knowledge gap document [14] highlighted the necessity of further characterizing this uncertainty, and called for new studies focused on measuring the tissue conductivities. In the LF range, most of the dosimetric investigations [12], [13], [15]–[18] used the values employed by Dimbylow in two studies that were used as a basis for developing the ICNIRP guidelines [6], [7]. This set of electrical conductivities was derived from a list of values for frequency below 100 Hz, which was published in a technical report released by Gabriel [19] after a series of investigations in the field [20]–[22]. Other works [5], [23] assigned the conductivity values based on a 4-Cole-Cole dispersion model meant for higher frequencies [22], which was also included in the technical report [19]. Herein, we investigated whether these two data sets produced significantly different electric field strengths in the brain.

Most of the conductivity values in Gabriel's investigations were derived from measurements on excised and post-mortem tissues. However, these samples are characterized by a different electrolyte concentration in respect to live tissues, which might affect the estimation of electrical conductivity [24], [25]. In this context, higher conductivity values than those reported in [6] and [22] were obtained for the white and grey matter following *in vivo* measurements during brain surgery [26]. New advanced non-invasive methods based on *in vivo* measurements, such as electrical impedance tomography (EIT) and Magnetic Resonance EIT (MREIT), seem to confirm higher electrical conductivity values for brain tissues [27]. An extensive meta-analysis review of the latest papers on human head electrical conductivities was recently conducted in [27], which showed higher values than those widely used in low-frequency dosimetry.

Hence the aim of this research was to characterize the effect of uncertainty in tissue properties on the electric field strengths induced in the brain. Twenty-five high-resolution head models were generated from magnetic resonance (MR) images. Electrical conductivities were then assigned to the tissues based on the values reported in three investigations, namely Dimbylow [6], Gabriel [22] and McCann [27]. The head models were exposed to uniform magnetic fields at 50 Hz along three different orthogonal directions (anterior-posterior, top-to-bottom and lateral). We selected the frequency of 50 Hz as it corresponds to the European power line frequency, and therefore it represents a common real-life exposure scenario. For this reason, most of the investigations in this field of research considered a frequency of 50 Hz [5], [6], [8], [16], [23], [29]. Please note that the conductivity ratios of the head tissues do not vary significantly up to frequencies of 100 kHz [28]. Therefore, the results obtained in the present study could be scaled within this frequency range [29]. Numerical calculations were performed with the purpose of estimating the variability of the calculated electric field strengths due to the uncertainty in the electrical conductivity of the tissues. In addition, a sensitivity analysis was conducted to evaluate which head tissue is mainly affected by electrical conductivity uncertainty when estimating the electric field strengths induced in the brain.

## II. MATERIALS AND METHODS

### A. PARTICIPANTS AND IMAGING METHODS

This investigation considered twenty-five participants who were recruited in a previous study [18]. The participants consisted of 12 males and 13 females (mean age $\pm$ standard deviation: 30 $\pm$ 6 years), who were scanned using a 3 T Magnetic Resonance Imaging (MRI) system (Magnetom Skyra; Siemens, Ltd., Erlangen, Germany) to obtain structural T1- and T2-weighted images. The Magnetization Prepared Rapid Acquisition in Gradient Echo (MPRAGE) sequence was used to acquire the structural T1-weighted images (TR = 2530 ms, TE = 3.3 ms, TI = 1100 ms, FA = 7°, FOV = 256 mm, voxel size = 1 × 1 × 1 mm, slice number = 176). For each participant, T2-weighted images were also obtained (TR = 3200 ms, TE = 412 ms, FA = 120°, FOV = 256 mm, voxel size = 1 × 1 × 1 mm, slice number = 176).

### B. HUMAN MODELS

FreeSurfer [30], [31] was used to process the structural T1-weighted images to segment the brain tissues. A semi-automatic procedure [32] was employed to improve the segmentation of the subcortical structures. In addition, our in-house segmentation pipeline processed T1- and T2-weighted images to segment the other non-brain tissues, i.e., skin, skull and cerebrospinal fluid (CSF). The segmented head models were then voxelized using cubic elements with a resolution

**TABLE 1. Electrical conductivities (S/m) of the tissues at 50 Hz, and their ratio for the main tissues of the head (CSF:GM, GM:WM).**

| Tissue | Gabriel | Dimbylow | McCann |
|---|---|---|---|
| GM | 0.08 | 0.10 | 0.47 |
| WM | 0.05 | 0.06 | 0.22 |
| Cerebellar GM | 0.10 | 0.10 | 0.54 |
| Cerebellar WM | 0.05 | 0.06 | 0.22 |
| CSF | 2.00 | 2.00 | 1.71 |
| Brainstem | 0.05 | 0.06 | 0.22 |
| Compact bone | 0.02 | 0.02 | 0.005 |
| Spongy bone | 0.08 | 0.07 | 0.05 |
| Fat | 0.045 | 0.04 | 0.06 |
| Skin | $4.5 \times 10^{-4}$ | 0.10 | 0.41 |
| Muscle | 0.24 | 0.35 | 0.32 |
| Dura | 0.50 | 0.50 | 0.46 |
| Blood | 0.70 | 0.70 | 0.57 |
| CSF:GM | 25 | 20 | 3.6 |
| GM:WM | 1.6 | 1.7 | 2.1 |

of 0.5 mm. Subsequently, we assigned to each voxel an electrical conductivity based on the values tabulated in three studies, which will be referred from now on as Gabriel [22], Dimbylow [6] and McCann [27] data sets. Table 1 shows the conductivities of the head tissues derived from these investigations. Please note that in the frequency range, the total conductivity $\sigma^*$ is the complex quantity $\sigma^* = \sigma + j\omega\varepsilon$, where $\omega$ is the angular frequency, and $\sigma$ and $\varepsilon$ are the electrical conductivity and permittivity of the tissues, respectively. However, at low-frequencies, biological tissues can be considered purely resistive as the conductivity $\sigma$ exceeds the permittivity $\epsilon$ by several orders of magnitude [33]. Therefore, the displacement current can be neglected, i.e., $j\omega\varepsilon \ll \sigma$ [33].

### C. EXPOSURE SCENARIOS

Exposure of the anatomically realistic head models to spatially uniform magnetic fields was considered, as it represents the reference exposure scenario for both ICNIRP [1] and IEEE [2], [3]. As shown in Fig. 1, three different magnetic field directions were investigated: top-bottom (TOP), left-right (LAT), and antero-posterior (AP). The homogeneous magnetic flux density ($\mathbf{B}_0$) at 50 Hz was set to be equal to the the reference level defined by ICNIRP guidelines for occupational exposure (1 mT). This allowed to directly compare our results with those used as a basis to develop the ICNIRP guidelines [6]. In addition, the incident magnetic field directions (TOP, LAT and AP) were aligned with the anatomical axes of each individual using a previously described procedure [18].

### D. ELECTRIC FIELD MODELING

The total induced electric field $\mathbf{E}$ can be expressed as the sum of *primary* ($\mathbf{E}_1$) and *secondary* ($\mathbf{E}_2$) electric fields as follows:

$$\mathbf{E} = \mathbf{E}_1 + \mathbf{E}_2 = -\nabla\phi + j\omega\mathbf{A}, \tag{1}$$

where $\mathbf{A}$ is the magnetic vector potential and $\phi$ is the electric scalar potential. In the low-frequency range, the electromagnetic wavelength is much larger than the dimension of the human head (~6000 km at 50 Hz). As a consequence,

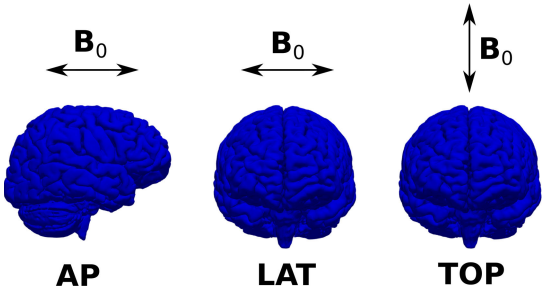


**FIGURE 1. Exposure of the brain to spatially uniform magnetic fields directed along AP, LAT and TOP directions.**

the time for the applied magnetic field to propagate in the head can be considered negligible. Therefore, the quasi-static approximation holds [33]. Under this assumption, the primary field $\mathbf{E}_1 = j\omega\mathbf{A}$ is due solely to the changing in the incident magnetic flux density $\mathbf{B}_0$. In the head model, the total electric field $\mathbf{E}$ generates a current density $\mathbf{J} = \sigma\mathbf{E}$, which produces an uneven distribution of charges at the interfaces of tissues with different conductivities, resulting in the *secondary* field $\mathbf{E}_2 = -\nabla\phi$. The latter depends solely on the contrast in the electrical conductivity of two adjacent tissues, and it is proportional to the magnitude of the normal component of the *primary* electric field [35], [36]. As a result, the electric field is enhanced in the low conductivity tissue and reduced in the high conductivity region [37]. This effect is maximum when the applied electric field is orthogonal to the interface, and for large contrast in the electrical conductivity values. Depending on these factors, electric field hot spots can be observed at the interfaces of tissues with different conductivities. It follows that the distribution of the electric field strengths strongly depends on the electrical conductivity values.

### E. FINITE ELEMENT METHOD

Under the quasi-static approximation [33], the scalar potential $\phi$ induced by the external magnetic field satisfies:

$$\begin{cases} \nabla \cdot \sigma\nabla\phi = j\omega\nabla \cdot \sigma\mathbf{A} & \text{in } \Omega \\ \mathbf{n} \cdot (\nabla\phi - j\omega\mathbf{A}) = 0 & \text{on } \partial\Omega, \end{cases} \tag{2}$$

where $\Omega$ is the domain of the solution (i.e., the head model), $\partial\Omega$ the boundary of $\Omega$, and $\mathbf{n}$ the normal vector of the surface $\partial\Omega$. For spatially uniform applied magnetic fields, the relationship between $\mathbf{A}$ and $\mathbf{B}_0$ can be expressed by:

$$j\omega\mathbf{A}(\mathbf{r}) = \frac{j\omega}{2}\mathbf{B}_0 \times \mathbf{r} \tag{3}$$

where $\mathbf{r}$ is the displacement vector from the direction of $\mathbf{B}_0$. Thus, the magnetic vector potential $\mathbf{A}$ was calculated analytically through (3). Then, to numerically determine $\phi$, (2) was solved using the finite-element method (FEM) with trilinear node-based basis functions in cubical elements [34]. Our solver was implemented in Matlab (MathWorks Inc., Natick, MA) and C programming language. The matrix equation resulting from discretization was solved iteratively using the geometric multigrid method with successive

over-relaxation [34]. The iteration stopped when a residual norm lower than $10^{-6}$ was reached. Once $\phi$ was determined at the vertices of the cubical grid, the total induced electric field was finally calculated from (1). Numerical simulations were performed for each participant and for each conductivity data set.

### F. POST-PROCESSING OF ELECTRIC FIELD DATA

The induced electric field was computed in the following brain tissues: cerebral grey matter (GM), nuclei (including various deep grey matter structures), cerebral white matter (WM), cerebellar GM, cerebellar WM, brainstem and eyes (approximating the retina). We also calculated the electric fields in the other non-brain tissues, such as skin, skull and CSF. Averaging was then performed over $2 \times 2 \times 2$ mm$^3$ cubes [1]. Voxels having an averaging volume extending beyond the boundary of the tissues were not considered [1]. To remove the effect of numerical artifacts (i.e., staircasing approximation error), the 99th percentile of the ICNIRP-averaged electric field was calculated for each tissue compartment [1]. As done in previous investigations [6], [18], the maximum electric field strength in the brain was calculated as the highest 99th percentile value over all the central nervous system (CNS) tissues ($E_{99}$). For completeness, we also derived the 99.9th, 99.99th percentiles together with the highest value (100th percentile) of the ICNIRP-averaged electric fields induced in the main tissues of the head. However, these results will be provided in a separate section (Appendix A), as in the following analysis we will only refer to the $E_{99}$ values. Please note that IEEE recommends averaging the induced electric field over an arbitrarily oriented segment of 5 mm length [2], [3], which does not differ significantly from the averaging scheme defined by ICNIRP [49].

### G. STATISTICAL ANALYSIS

The $E_{99}$ values were statistically analyzed using the open-source programming language `R` (version 3.6.2). For each exposure scenario, a Welch's ANOVA test was performed to check whether there was statistically significant difference between the means of the $E_{99}$ values among the different conductivity data sets. To compare the means we used a F-test with a level of statistical significance of 0.05. Games-Howell post-hoc test was then performed to compare the average $E_{99}$ values for all the possible combinations of the conductivity data sets.

### H. SENSITIVITY ANALYSIS

A sensitivity analysis was performed to determine how the changes in the electrical conductivity of the head tissues affected the $E_{99}$ values. For each data set and exposure scenario, we varied the conductivity of one tissue at a time, while keeping the others to their baseline value. The range of conductivity variation for each head tissue was approximately set from the minimum to the maximum value across all the data sets (Table 1). At each conductivity increase, the $E_{99}$ value was calculated and then averaged across the participants.

**TABLE 2. Statistical data of the highest 99th percentile of the ICNIRP-averaged electric fields over all the brain tissues (mV m$^{-1}$) derived for each conductivity data set, along with the mean value and standard deviation with the corresponding 95% confidence interval in brackets extracted from the normal distributions. Minimum and maximum values are also reported.**

| | Gabriel data set | | |
|---|---|---|---|
| | AP | LAT | TOP |
| Minimum | 16.6 | 18.2 | 16.0 |
| Mean [CI] | 18.4 [17.9, 18.9] | 20.8 [20.1, 21.5] | 17.9 [17.4, 18.3] |
| SD [CI] | 1.2 [0.9, 1.6] | 1.7 [1.3, 2.3] | 1.0 [0.8, 1.4] |
| Maximum | 20.8 | 25.6 | 19.7 |
| | Dimbylow data set | | |
| | AP | LAT | TOP |
| Minimum | 16.6 | 19.6 | 15.4 |
| Mean [CI] | 18.2 [17.7, 18.7] | 22.0 [21.3, 22.7] | 17.2 [16.8, 17.6] |
| SD [CI] | 1.2 [0.9, 1.7] | 1.7 [1.3, 2.4] | 1.0 [0.8, 1.4] |
| Maximum | 21.0 | 26.3 | 18.9 |
| | McCann data set | | |
| | AP | LAT | TOP |
| Minimum | 13.4 | 14.0 | 13.9 |
| Mean [CI] | 14.3 [14.0, 14.6] | 15.5 [15.1, 15.7] | 15.2 [14.9, 15.5] |
| SD [CI] | 0.7 [0.6, 1.0] | 0.8 [0.6, 1.1] | 0.7 [0.6, 1.0] |
| Maximum | 16.2 | 16.8 | 16.7 |

## III. RESULTS

Fig. 2 shows a comparison between the induced electric field distributions in each of the different data sets for a representative voxelized head model. The results were derived for uniform magnetic field (1 mT) exposure at 50 Hz in the AP, LAT and TOP directions. Electric field maps showing the differences in the results are also reported. By visual inspection, it is clear that Gabriel and Dimbylow data sets provided analogous electric field distributions, given their electrical conductivities being rather similar. However, the conductivity values were notably different in the McCann data set, which indeed produced considerably dissimilar induced electric fields.

Box-plots in Fig. 3 provide the variability among the individuals of the $E_{99}$ values for each data set, together with pie-charts representing the percentage of tissues where these highest strengths were found.

For each exposure direction and within each conductivity data set, the variability of the $E_{99}$ values followed a normal distribution, according to Shapiro normality test ($p > 0.05$). For each distribution, we determined the mean value across the participants and the standard deviation (SD), together with the 95% confidence interval (CI). Results are shown in Table 2, which also includes the minimum and maximum values of the distributions. Welch's ANOVA test revealed a statistically significant difference between the $E_{99}$ mean values derived for each data set in the case of TOP [$F(2, 47) = 63.2$, $p = 5 \times 10^{-14}$], LAT [$F(2, 41.3) = 221.5$, $p = 2 \times 10^{-16}$], and AP [$F(2, 45.3) = 161.5$, $p = 2 \times 10^{-16}$] exposures. Post-hoc pairwise comparisons was also performed to asses which pairs of means were significantly different from each other. Results are included in the box-plots of Fig. 3.

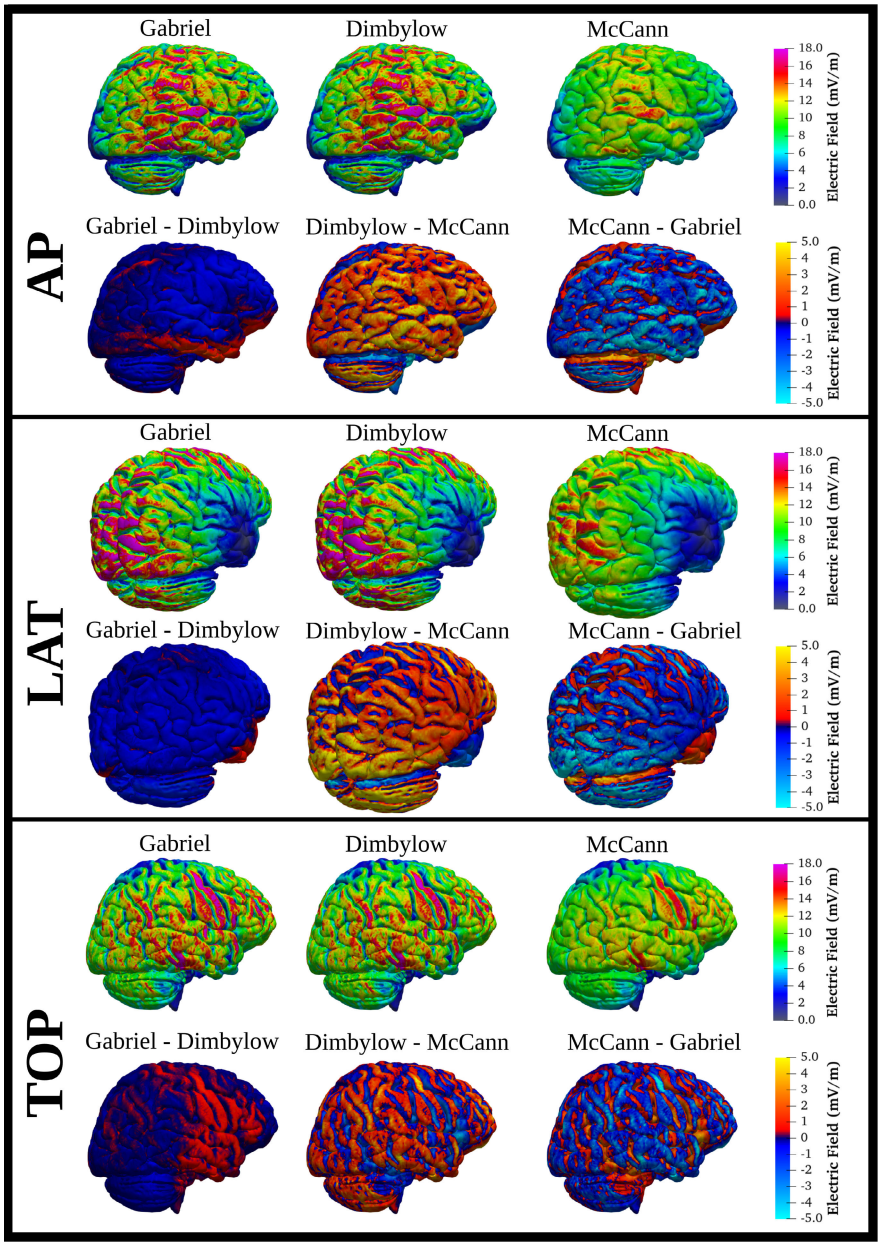


**FIGURE 2.** Electric field strengths induced in the brain of a representative participant for three different conductivity data sets (Gabriel, Dimbylow and McCann). Relative differences in the results are also shown. The magnetic flux density was set to be equal to the reference level for ICNIRP occupational exposure (1 mT), and directed along three different directions (TOP, LAT and AP).

Overall, the McCann data set produced statistically lower $E_{99}$ values (Fig. 3) due to its higher conductivities of the brain tissues (i.e., GM and WM) compared to the ones of Gabriel and Dimbylow. The peak strengths always occurred in the WM, where the induced electric field was enhanced by the GM/WM conductivity ratio being the highest among the data sets (see Appendix A).

No significant differences were found between the Gabriel and Dimbylow data sets, except for the LAT exposure where the former gave slightly higher $E_{99}$ values due to the stronger intensities produced posteriorly in the cerebellar GM (see Appendix A). Despite statistical significance, this difference was only 1.2 [0.02, 2.34] mV $m^{-1}$. In this context, the highest $E_{99}$ values were always observed when the magnetic flux density was oriented in the lateral direction (Fig. 3), due to the larger cross-section area in the sagittal plane of the head [17]. Moreover, the LAT exposure mainly involved posterior regions of the brain (Fig. 3). In the Gabriel and Dimbylow data sets, this explains why the cerebellar GM was found to be the tissue characterized by the highest strengths most of times. For the other exposure scenarios, the Gabriel data set resulted in having the maximum strengths always in

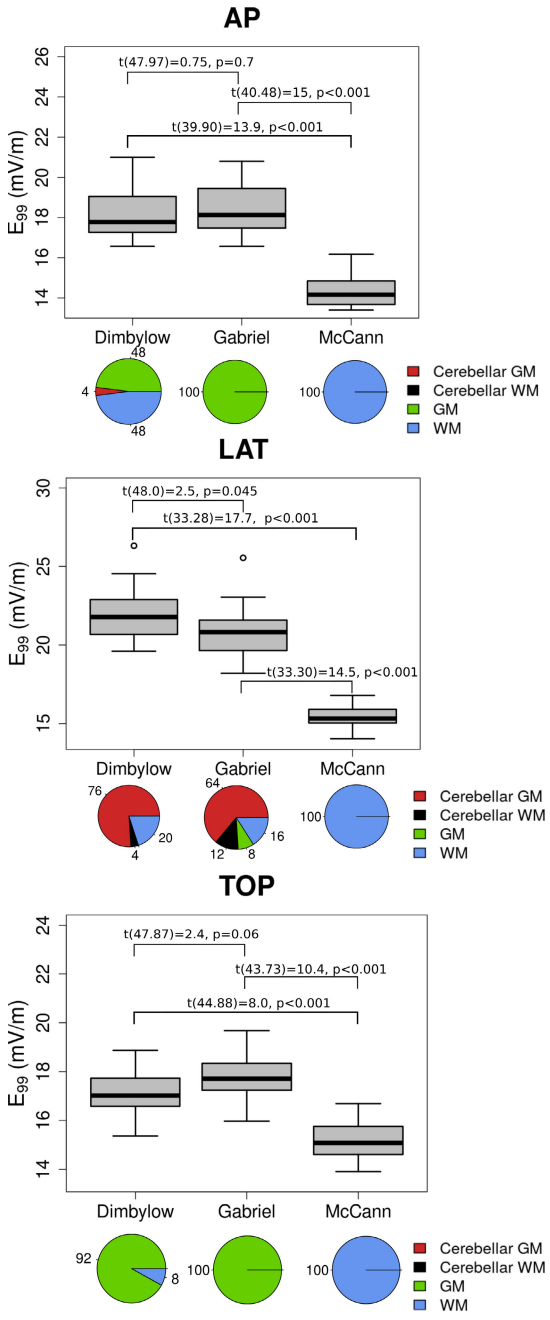


**FIGURE 3.** The boxplots show the variation of the $E_{99}$ values among the individuals for the different exposure scenarios and the electrical conductivity data sets. The pie-charts indicate the percentage of brain tissues exhibiting the maximum electric field strengths. In addition, the boxplots contain the results from the Games-Howell post-hoc test, that was used to identify which differences between pairs of means were significant.

the GM (Fig. 3), given the combination of its high CSF/GM conductivity ratio and low GM/WM conductivity ratio that enhanced the electric fields in the GM. On the other hand, the Dimbylow data set had a lower CSF/GM conductivity ratio, which reduced the strengths in the GM, and by a higher GM/WM conductivity ratio, which instead enhanced the strengths in the WM (see Appendix A). For this reason, the Dimbylow data set resulted in having also the WM as the compartment characterized by the highest electric field strengths (Fig. 3).

### A. SENSITIVITY ANALYSIS

In the following sections, we present the results obtained when studying how the $E_{99}$ values were affected by changes in the electrical conductivity of the head tissues. This analysis was carried out by varying the electrical conductivity of one tissue at a time while keeping the others to their baseline values. Results were averaged across all the participants. To have a better insight regarding the trend of the sensitivity curves, Appendix B provides the 99th percentile electric fields calculated separately in the main brain tissues, including the CSF. As the LAT direction gave the highest electric field strengths, we focused the sensitivity analysis mainly on this exposure scenario.

#### 1) EFFECT OF GM CONDUCTIVITY

Fig. 4 (a) shows the variation of the $E_{99}$ values as a function of the GM conductivity, which was varied in each data set from 0.07 S/m to 0.47 S/m. As revealed in Fig. 7 of Appendix B, the electric field strengths decreased in the GM and increased in all the other compartments as the GM conductivity was augmented.

Considering the McCann data set, for rather small values of the GM conductivity, the induced electric field strengths in the GM were the highest (Fig. 7 of Appendix B). This followed from the GM being surrounded by two tissues with higher conductivity (i.e., WM and CSF), that enhanced the field intensities in the GM. However, as the GM conductivity increased, the higher conductivity ratio GM/WM produced weaker fields in the GM and stronger fields in the WM. As a result, at some point the electric field strengths in the WM became higher than that of the GM. Therefore, the $E_{99}$ values first lowered for the effect of the GM which experienced decreasing fields, and then they rose due to the increasing strengths in the WM (Fig. 4 (a)).

For the considered range of GM conductivity, the initial decreasing phase was not observed in the Gabriel and Dimbylow data sets due to the high intensities produced posteriorly in the cerebellar GM (Fig. 7 of Appendix B).

#### 2) EFFECT OF WM CONDUCTIVITY

Fig. 4 (b) provides the variations of the $E_{99}$ values when the WM and cerebellar WM conductivities were varied from 0.05 S/m to 0.265 S/m. In the McCann data set, the WM conductivity always remained much smaller than that of the other tissues. This produced the highest strengths in the WM, which decreased as the WM conductivity increased (Fig. 7 of Appendix B). As a consequence, the $E_{99}$ values followed the decreasing changes in the electric field strengths induced in the WM (Fig. 4 (b)).

For the other data sets, the WM conductivity started exceeding that of the other brain tissues at the very beginning of the conductivity interval. As a result, an overall rise in the

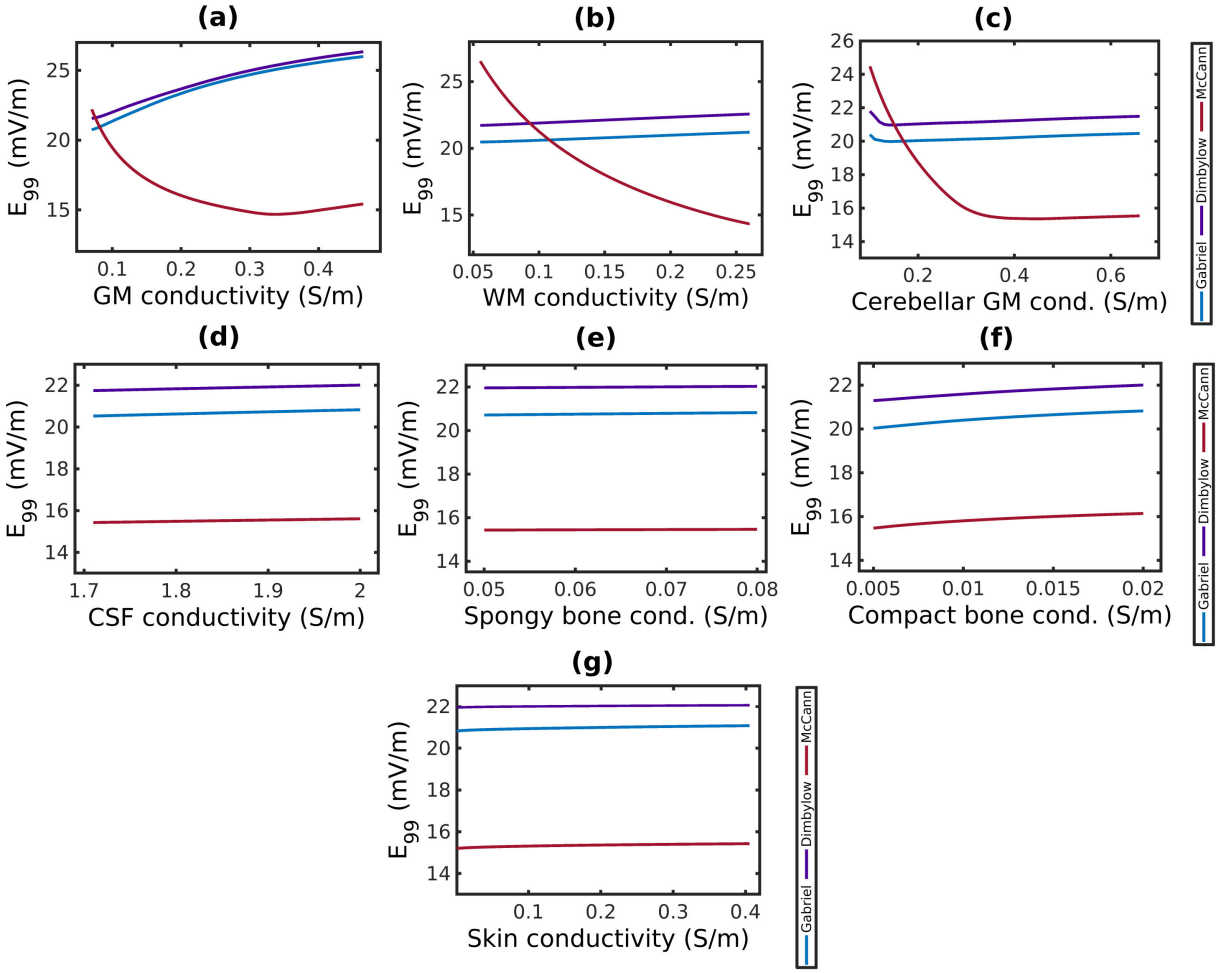


**FIGURE 4.** The highest 99th percentile values of the ICNIRP-averaged electric fields over all the brain tissues as a function of the conductivity of (a) GM, (b) WM, (c) cerebellar GM, (d) CSF, (e) spongy bone, (f) compact bone and (g) skin. Results were derived for the LAT exposure scenario, and data were averaged across the individuals.

$E_{99}$ values was observed due to the increasing strengths in the cerebellar GM (Fig. 7 of Appendix B).

### 3) EFFECT OF CEREBELLAR GM

Fig. 4 (c) reports the $E_{99}$ values determined when the cerebellar GM conductivity was varied from 0.1 S/m to 0.66 S/m. As the LAT exposure produced the highest electric fields posteriorly to the brain, the electric field strengths in the cerebellar GM resulted to be rather high, especially when its conductivity was small compared to the one of the other compartments. As the conductivity was increased, the field strengths decreased in the cerebellar GM, whereas they increased in the GM and the WM, the latter experiencing the highest strengths (Fig. 7 of Appendix B). Therefore, the $E_{99}$ values first lowered for the decreasing strengths in the cerebellar GM, and then they rose due to the increasing strengths in the WM.

### 4) EFFECT OF CSF

The conductivity of the CSF was quite consistent among the investigations, therefore its change from 1.71 S/m to 2 S/m resulted in a steady and modest increase in the $E_{99}$ values (Fig. 4 (d)). In the McCann data set, this augmentation followed the changes in the WM, which experienced the highest strengths due to its lowest conductivity value (Fig. 7 of Appendix B). In the other data sets, the changes in the $E_{99}$ values were mainly due to the increasing strengths produced in the cerebellar GM.

### 5) EFFECT OF SPONGY BONE AND COMPACT BONE

As in the case of the CSF, the conductivity of the spongy bone did not vary considerably among the data sets. Therefore, its change from 0.05 S/m to 0.08 S/m did not affect significantly the $E_{99}$ values (Fig. 4 (e)). However, a steady increase was observed when the compact bone conductivity was varied from 0.005 S/m to 0.02 S/m (Fig. 4 (f)). As shown in Fig. 7 of Appendix B, the $E_{99}$ values followed the changes in the increasing strengths induced in the cerebellar GM (Gabriel and Dimbylow data sets) and in the WM (McCann data set).

### 6) EFFECT OF SKIN

The electrical conductivity of the skin was varied from 0.00045 S/m to 0.41 S/m. In the McCann data set, these

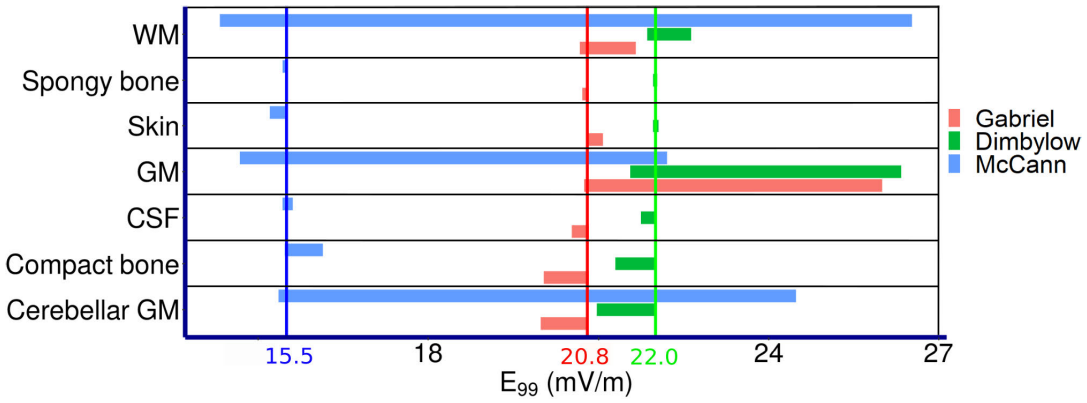


**FIGURE 5.** Range bar plots showing the variation between the minimum and maximum electric field strengths derived from the sensitivity curves. Vertical lines represent the average peak strengths obtained with the baseline conductivity values.

changes produced a rather small increase in the $E_{99}$ values (Fig. 4 (g)) due to variations in the WM (Fig. 7 of Appendix B). A weak increase was also observed in the Gabriel and Dimbylow data sets, produced by the changes in the cerebellar GM (Fig. 7 of Appendix B).

## IV. DISCUSSION

This study extensively investigated the effect of the uncertainty in the electrical conductivity of the head tissues on the electric field strengths induced in the brain of twenty-five individuals who were exposed to spatially uniform magnetic fields at 50 Hz. The incident fields were set to be equal to the ICNIRP reference level for occupational exposure (1 mT) and directed along the LAT, AP and TOP directions. The electric fields were computed by assigning three different conductivity values to the head tissues based on the studies of Dimbylow [6], Gabriel [22] and McCann [27]. The overall maximum strengths in the brain ($E_{99}$ values) were then evaluated as the highest 99th percentile value among the brain tissues of the electric fields averaged over $2 \times 2 \times 2$ mm$^3$ cubes [1]. For the sake of clarity, Appendix A includes the 99.9th, 99.99th, and 100th percentile values calculated in the main tissues of the head. An additional analysis was also conducted to study the sensitivity of the $E_{99}$ values to electrical conductivity variations. To our knowledge, this is the first study of its kind for spatially uniform magnetic fields at 50 Hz, although several researches were conducted in the case of non-invasive brain stimulation for a limited number of spherical [35] and realistic head models [38], [39]. Our intent was to characterize how the uncertainty in tissue properties affect the electric strengths induced in the brain, with the purpose of providing quantitative data useful for the revision of the human exposure guidelines to electromagnetic fields at low frequencies.

Based on an extensive review of the latest research concerning human head tissue properties, McCann [27] estimated higher values of electrical conductivities for the brain tissues than those commonly employed in the low-frequency range [6], [22]. This had a major effect on the numerical results: the higher the electrical conductivities of the brain tissues, the lower the induced electric field strengths in the brain (Fig. 3). In particular, the McCann data set produced an average peak strength of $15.5 \pm 0.8$ mV m$^{-1}$ for LAT exposure, which was found to be significantly lower than the ones produced by Gabriel ($20.8 \pm 1.7$ mV m$^{-1}$) and Dimbylow ($22.0 \pm 1.7$ mV m$^{-1}$) data sets. Significantly lower peak electric fields were also found for the other exposure scenarios (Table 2). No statistically significant difference was observed between Gabriel and Dimbylow, with the only exception for LAT exposure where they differ only of 1.2 [0.02, 2.34] mV m$^{-1}$.

Please note that the present investigation considered a limited number of twenty-five participants. However, the rather narrow confidence intervals provided in Table 2 suggest that the considered sample size is adequate to represent a larger population. In this context, the results derived here using the Dimbylow data set are in good accordance with a recent study which recruited a larger population consisting of 118 individuals [18].

To easily compare our results with the limits defined by the safety standard/guidelines, Table 3 reports the obtained average induced electric field strengths divided by the ICNIRP and IEEE exposure factors, i.e., the ratio between the basic restriction/dosimetric reference limit and the corresponding (exposure) reference level. Values higher than 1 indicate that the limits are exceeded. As shown in Table 3, for each exposure scenario and conductivity data set, the average induced electric field strengths were always in compliance with the ICNIRP occupational basic restrictions for the CNS tissues (100 mV m$^{-1}$) [1]. ICNIRP derived its CNS induction factor from dosimetric calculations that used only one anatomical model (NORMAN), based on a study which employed the Dimbylow data set [6]. In this investigation, a maximum induced electric field strength in the brain equal to 33.0 mV m$^{-1}$ per mT was found for LAT exposure. The value of 1 mT was set as the occupational exposure reference level at 50 Hz for the CNS tissues, as it would produce the corresponding basic restriction of $3 \cdot 33.0$ mV m$^{-1}$ = 100 mV m$^{-1}$, where 3 represents a reduction factor accounting for dosimetric uncertainty. However, the results derived

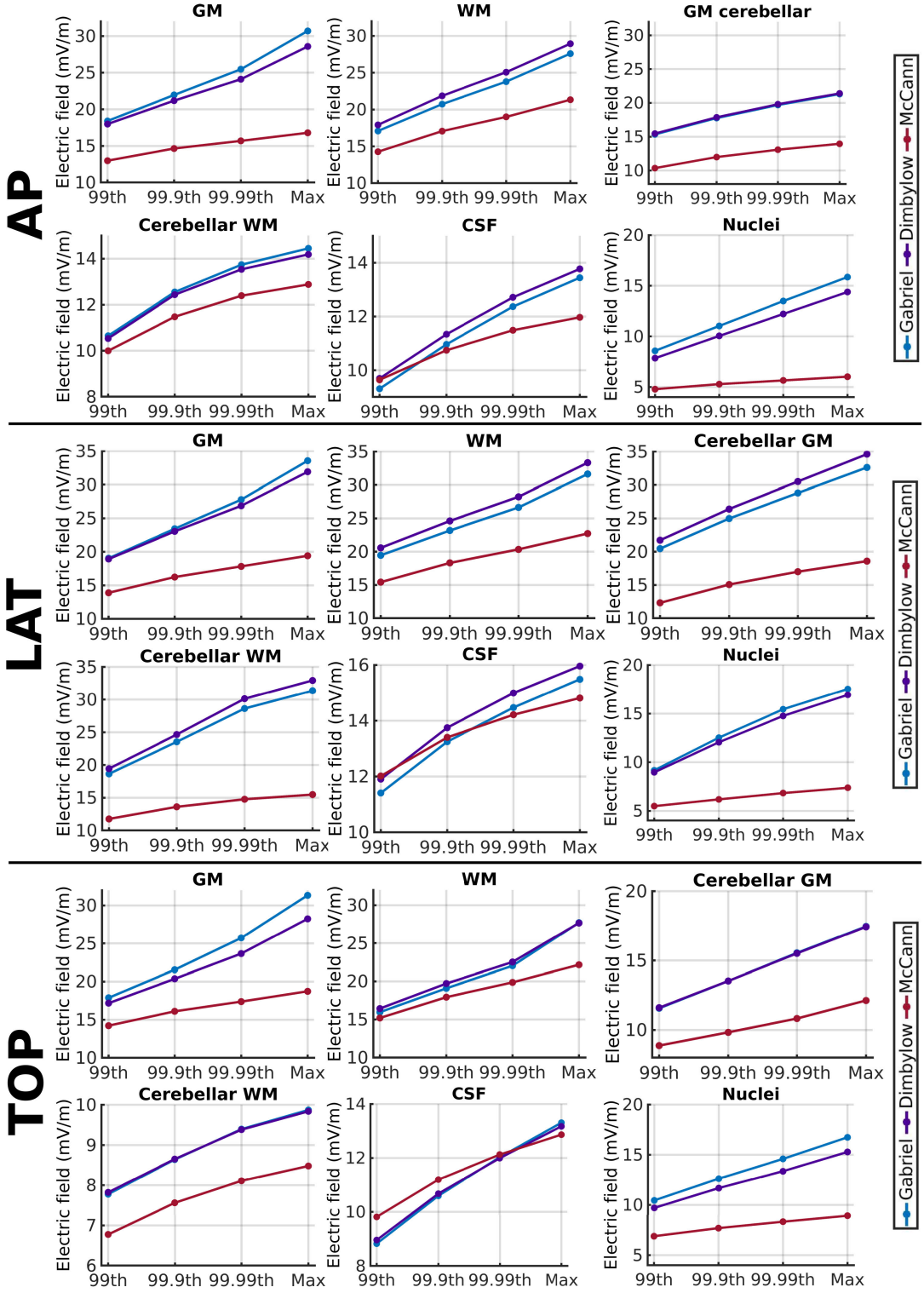


**FIGURE 6.** 99th, 99.9th, 99.99th and 100th percentile values of the ICNIRP-averaged electric field for different tissues of the head. Exposure to 1 mT magnetic flux density at 50 Hz along the AP, LAT and TOP directions.

here using the Gabriel and Dimbylow data sets were 37% and 33% lower than the above value used as basis for developing the ICNIRP guidelines [1], [6]. Considering the identical (Dimbylow) or rather similar (Gabriel) conductivity values, these differences can be explained by the lower resolution (approximately 2 mm) used in [6], that can overestimate the electric fields compared to finer resolutions [17]. Regarding the McCann data set, this difference becomes even more

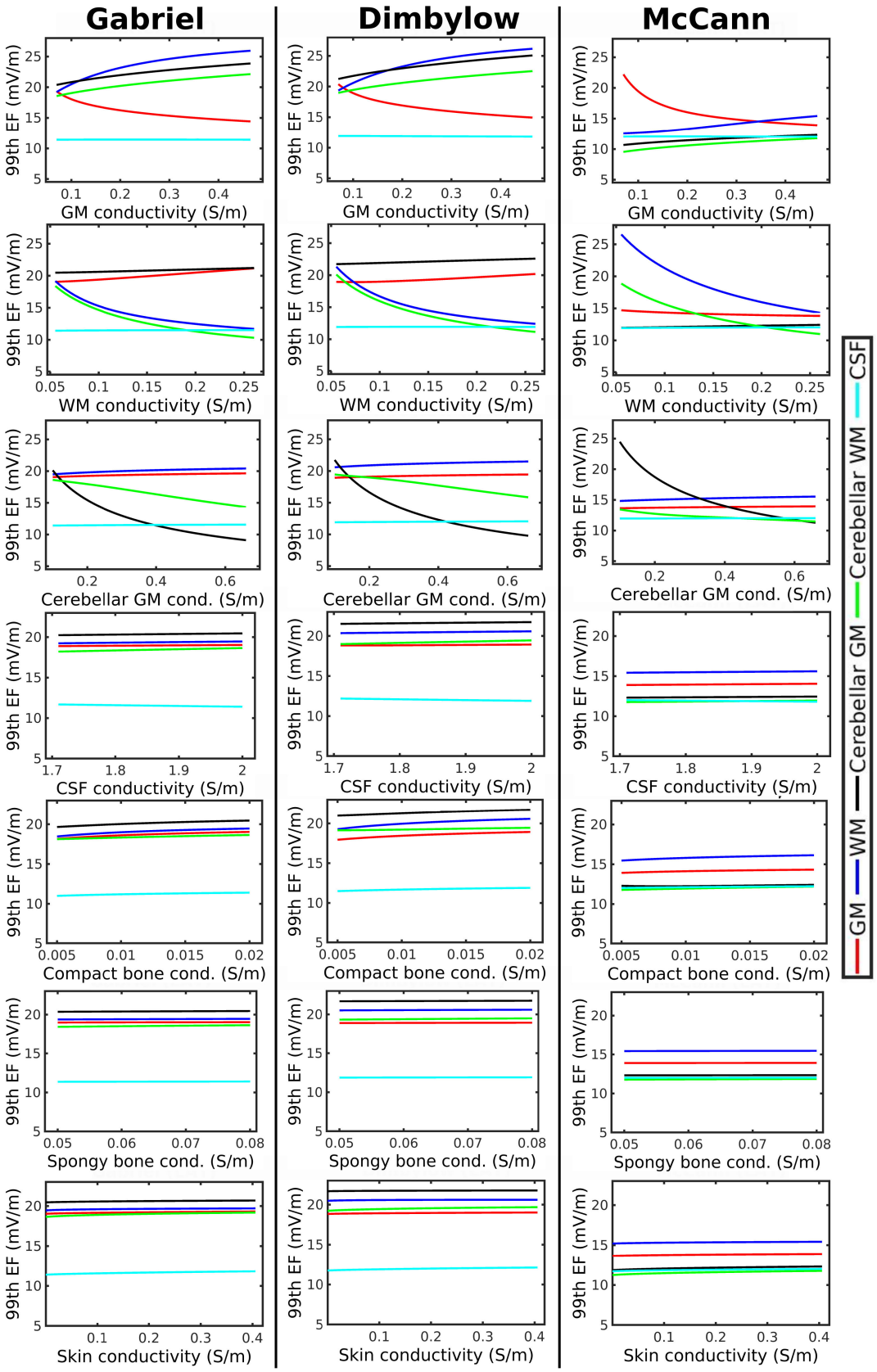


**FIGURE 7.** Variation of the 99th percentile electric fields in the main tissues of the head as a function of the conductivity of GM, WM, cerebellar GM, CSF, compact/spongy bone and skin. Data were derived for LAT exposure and averaged across the participants.

**TABLE 3.** Ratio of the average induced electric field strengths to the ICNIRP (100 mV $m^{-1}$ per mT) and IEEE (16.33 mV $m^{-1}$ per mT) exposure factors. The exposure factors were derived from the limits defined by ICNIRP and IEEE for occupational exposure and people in unrestricted environment, respectively.

| | LAT | | |
|---|---|---|---|
| | Gabriel | Dimbylow | McCann |
| ICNIRP | 0.21 | 0.22 | 0.15 |
| IEEE | 1.27 | 1.35 | 0.95 |
| | AP | | |
| | Gabriel | Dimbylow | McCann |
| ICNIRP | 0.18 | 0.18 | 0.14 |
| IEEE | 1.13 | 1.11 | 0.88 |
| | TOP | | |
| | Gabriel | Dimbylow | McCann |
| ICNIRP | 0.18 | 0.17 | 0.15 |
| IEEE | 1.10 | 1.05 | 0.93 |

significant and it is in the order of 50%. As a result, the reference level derived with higher brain conductivity values would be approximately twice (∼2.15 mT) as high as that currently used, assuming that the same reduction factor of 3 would be applied.

In the IEEE standard [2], [3], the exposure reference levels were obtained from the dosimetric reference limits through a homogeneous elliptical model. For people in unrestricted environment, the corresponding IEEE exposure factor is equal to 16.33 mV $m^{-1}$ per mT, which slightly exceeds the values derived here using the McCann data set. Therefore, the higher brain conductivity values lowered the discrepancies between the maximum electric field strengths obtained in the ellipsoidal and realistic anatomical models. As a result, for each exposure scenario, the average electric field strengths obtained with the McCann data set were always in compliance with the limits defined by IEEE for people in unrestricted environment (Table 3). On the other hand, the results for Gabriel and Dimbylow data sets were approximately 27% and 35% higher than the IEEE exposure factor. In this case, the limits were therefore exceeded (Table 3).

Fig. 5 offers a simple visual representation of our sensitivity analysis results, showing that changes in the conductivity of the brain tissues had a major impact on the peak electric field strengths induced in the brain. The horizontal bars represent the range between the minimum and maximum values of the peak strengths derived from the sensitivity curves, whereas the vertical lines correspond to the average strengths obtained with the baseline conductivity values (Table 2). The lower the conductivity of a brain tissue, the higher the maximum electric field strength induced in that tissue, and vice versa. Therefore, when the conductivity of a brain tissue was varied from a minimum to a maximum value, the electric field strength decreased in the compartment affected by an increase in the conductivity, whereas it increased in the other ones (see Appendix B). If the minimum value of the conductivity interval was much smaller than the conductivity of the other brain tissues, an initial rapid decrease of the $E_{99}$ values was observed for the effect of lowering strengths induced in the compartment whose conductivity was augmented. When the conductivity became sufficiently higher than that of the other brain tissues, a steady augmentation followed due to the surrounding compartments experiencing increased field strengths. Changes in the non-brain tissue conductivities (i.e., skull, CSF and skin) marginally affected the overall electric field strengths (Fig. 5). Please note that the range of variation of CSF conductivity was quite small, since its estimated value is consistent among different investigations [22], [27], [40].

The effect of age related changes in the conductivity of the brain tissues on the electric field strengths needs to be further investigated. With aging, the brain undergoes to structural and chemical changes resulting in less water content [41]. Experiments on rats demonstrated that dielectric property of brain tissues decreased with age [42], [43]. As a consequence, the conductivity of the brain tissues in the young population is expected to be higher, leading to possibly lower field strengths. Future studies should also include the anisotropy of the brain tissues. In this context, GM was proven to be isotropic [45]. On the other hand, WM exhibits anisotropic properties, i.e., its conductivity depends on the orientation of the fibers [45]. In particular, the conductivity along the fibers is higher than that directed in the perpendicular direction [46], [47]. Therefore, the WM conductivity becomes a tensor, which might produce a scaling and/or rotation of the induced electric field in respect to the case the WM was isotropic. This effect on the electric field strengths induced in the brain requires further investigation. However, inclusion of the anisotropy properties of the WM into numerical methods, as well as those of any other tissue, represents a rather challenging and complicated task. One major problem in computational dosimetry consists in assigning the orientation of the nerve fibers. A rigorous assessment of the effect of anisotropy should include individual high-resolution head models where the WM conductivity anisotropy is modeled from diffusion tensor imaging (DTI) [27]. This approach was used in an investigation conducted by De Lucia et al [48] for transcranial magnetic stimulation, where the authors showed that anisotropy leaded to differences up to 10% in the maximum induced field. However, this represents a localized exposure scenario, which is rather different from that of uniform magnetic field exposure. Please note that other sources of uncertainty, such as computational dosimetry and variability among individuals, were extensively investigated in our previous works [17], [18].

## V. CONCLUSION

We studied the variability of the electric field strengths induced in the brain due to uncertainty in the electrical conductivity of the tissues. For this purpose, we employed commonly-used sets of low-frequency conductivity data, as well as new values based on an extensive meta-analysis review of the latest papers in this field. The new estimates of the brain conductivity values, which were considerably higher that those widely used in low-frequency dosimetry, produced significantly weaker electric field strengths. The latter were up to 50% lower than the peak electric field

strength used as basis for developing the ICNIRP guidelines. On the other hand, the elliptical exposure model used in the IEEE standard would produce rather comparable electric field strengths to those obtained using anatomical models employing higher brain electrical conductivities.

A large variability in the tissue electrical conductivity values is still present in literature. In this context, our sensitivity analysis showed that variations in the GM, WM and cerebellar GM conductivity values had a major effect on the electric field strengths induced in the brain. More studies focused on measuring the dielectric properties of brain tissues are needed to provide accurate and realistic conductivity data. This would certainly contribute to improving the accuracy of low-frequency dosimetric studies.

The present investigation provides quantitative data that will be useful for the next revision of the safety exposure guidelines/standard for human protection to electromagnetic fields. Our results are intended to characterize the variability of the electric field strengths induced in the brain due to uncertainty in the electrical conductivity values. We believe that these data could be useful for the selection of appropriate reduction factors for deriving exposure reference levels that will not be overly protective for the human population.

## APPENDIX A
## PERCENTILE VALUES OF THE ICNIRP-AVERAGED ELECTRIC FIELDS IN THE MAIN TISSUES OF THE HEAD

Fig. 6 shows the 99th, 99.9th and 99.99th percentiles along with the highest electric field strengths (100th percentile) derived from different tissues of the head after averaging the electric field over $2 \times 2 \times 2$ mm$^3$ cubes. Results refer to uniform exposure to 1 mT magnetic flux density at 50 Hz along the AP, LAT and TOP directions. Data were averaged across the participants.

## APPENDIX B
## SENSITIVITY RESULTS FOR THE MAIN TISSUES OF THE HEAD

Fig. 7 show the variation of the 99th percentile values of the ICNIRP-averaged electric fields as a function of the electrical conductivity of several head tissues. Results were derived for uniform exposure to 1 mT magnetic flux density at 50 Hz directed along the LAT direction. Data were averaged across the participants.

## REFERENCES

[1] ICNIRP, "Guidelines for limiting exposure to time-varying electric and magnetic fields (1 Hz to 100 kHz)," *Health Phys*, vol. 99, no. 6, pp. 818–836, 2010, doi: 10.1097/HP.0b013e3181f06c86.

[2] *IEEE Standard for Safety Levels with Respect to Human Exposure to Electromagnetic Fields, 0-3 kHz*, Standard C95.6-2002, Institute of Electrical and Electronics Engineers, New York, NY, USA, 2002, doi: 10.1109/IEEESTD.2002.94143.

[3] *IEEE Standard for Safety Levels With Respect to Human Exposure to Electric, Magnetic, and Electromagnetic Fields, 0 Hz to 300 GHz*, Standard C95.1-2019, Institute of Electrical and Electronics Engineers, New York, NY, USA, 2019, doi: 10.1109/IEEESTD.2019.8859679.

[4] *Extremely Low Frequency Fields; Environmental Health Criteria Monograph, 238*, World Health Org., Geneva, Switzerland, 2007.

[5] J. F. Bakker, M. M. Paulides, E. Neufeld, A. Christ, X. L. Chen, N. Kuster, and G. C. van Rhoon, "Children and adults exposed to low-frequency magnetic fields at the ICNIRP reference levels: Theoretical assessment of the induced electric fields," *Phys Med Biol*, vol. 57, no. 7, pp. 1815–1829, 2012, doi: 10.1088/0031-9155/57/7/1815.

[6] P. Dimbylow, "Development of the female voxel phantom, NAOMI, and its application to calculations of induced current densities and electric fields from applied low frequency magnetic and electric fields," *Phys. Med. Biol.*, vol. 50, no. 6, pp. 1047–1070, 2005, doi: 10.1088/0031-9155/50/6/002.

[7] P. Dimbylow, "Development of pregnant female, hybrid voxel-mathematical models and their application to the dosimetry of applied magnetic and electric fields at 50 Hz," *Phys. Med. Biol.*, vol. 51, no. 10, pp. 2383–2394, 2006, doi: 10.1088/0031-9155/51/10/003.

[8] X.-L. Chen, S. Benkler, N. Chavannes, V. De Santis, J. Bakker, G. van Rhoon, J. Mosig, and N. Kuster, "Analysis of human brain exposure to low-frequency magnetic fields: A numerical assessment of spatially averaged electric fields and exposure limits," *Bioelectromagnetics*, vol. 34, no. 5, pp. 375–384, Jul. 2013, doi: 10.1002/bem.21780.

[9] P. Lövsund, P. Å. Öberg, and S. E. G. Nilsson, "Magneto-and electrophosphenes: A comparative study," *Med. Biol. Eng. Comput.*, vol. 18, no. 6, pp. 758–764, 1980, doi: 10.1007/BF02441902.

[10] P. Lövsund, P. Å. Öberg, S. E. G. Nilsson, and T. Reuter, "Magnetophosphenes: A quantitative analysis of thresholds," *Med. Biol. Eng. Comput.*, vol. 18, no. 3, pp. 326–334, 1980, doi: 10.1007/BF02443387.

[11] J. P. Reilly, *Applied Bioelectricity: From Electrical Stimulation to Electropathology*. New York, NY, USA: Springer, 1998.

[12] T. W. Dawson, K. Caputa, and M. A. Stuchly, "A comparison of 60 Hz uniform magnetic and electric induction in the human body," *Phys. Med. Biol.*, vol. 42, no. 12, pp. 2319–2329, Dec. 1997, doi: 10.1088/0031-9155/42/12/001.

[13] A. Hirata, K. Caputa, T. W. Dawson, and M. A. Stuchly, "Dosimetry in models of child and adult for low-frequency electric field," *IEEE Trans. Biomed. Eng.*, vol. 48, no. 9, pp. 1007–1012, 2001, doi: 10.1109/10.942590.

[14] ICNIRP, "Gap in knowledge to the," Guidelines for limiting exposure to time-varying electric and magnetic fields (1 Hz to 100 kHz)," *Health Phys.*, vol. 118, no. 5, pp. 533–542, 2020, doi: 10.1097/HP.0000000000001261.

[15] A. Hirata, K. Wake, S. Watanabe, and M. Taki, "*In-situ* electric field and current density in Japanese male and female models for uniform magnetic field exposures," *Radiat. Protection Dosimetry*, vol. 135, no. 4, pp. 272–275, 2009, doi: 10.1093/rpd/ncp117.

[16] A. Hirata, Y. Takano, O. Fujiwara, T. Dovan, and R. Kavet, "An electric field induced in the retina and brain at threshold magnetic flux density causing magnetophosphenes," *Phys. Med. Biol.*, vol. 56, no. 13, pp. 4091–4101, 2011, doi: 10.1088/0031-9155/56/13/022.

[17] M. Soldati and I. Laakso, "Computational errors of the induced electric field in voxelized and tetrahedral anatomical head models exposed to spatially uniform and localized magnetic fields," *Phys. Med. Biol.*, vol. 65, no. 1, Jan. 2020, Art. no. 015001, doi: 10.1088/1361-6560/ab5dfb.

[18] M. Soldati, T. Murakami, and I. Laakso, "Inter-individual variations in electric fields induced in the brain by exposure to uniform magnetic fields at 50 Hz," *Phys. Med. Biol.*, vol. 65, no. 21, Oct. 2020, Art. no. 215006, doi: 10.1088/1361-6560/aba21e.

[19] C. Gabriel, "Compilation of the dielectric properties of body tissues at RF and microwave frequencies," Armstrong Lab. (AFMC), Occupational Environ. Health Directorate, Radiofrequency Radiat. Division, Brooks Air Force Base, TX, USA, Tech. Rep. AL/OE-TR-1996-0037, 1996.

[20] C. Gabriel, S. Gabriel, and E. Corthout, "The dielectric properties of biological tissues: I. Literature survey," *Phys. Med. Biol.*, vol. 41, no. 11, pp. 2231–2249, 1996, doi: 10.1088/0031-9155/41/11/001.

[21] S. Gabriel, R. W. Lau, and C. Gabriel, "The dielectric properties of biological tissues: II. Measurements in the frequency range 10 Hz to 20 GHz," *Phys. Med. Biol.*, vol. 41, no. 11, pp. 2251–2269, 1996, doi: 10.1088/0031-9155/41/11/002.

[22] S. Gabriel, R. W. Lau, and C. Gabriel, "The dielectric properties of biological tissues: III. Parametric models for the dielectric spectrum of tissues," *Phys. Med. Biol.*, vol. 41, no. 11, pp. 2271–2293, 1996, doi: 10.1088/0031-9155/41/11/003.

[23] K. Aga, A. Hirata, I. Laakso, H. Tarao, Y. Diao, T. Ito, Y. Sekiba, and K. Yamazaki, "Intercomparison of *in situ* electric fields in human models exposed to spatially uniform magnetic fields," *IEEE Access*, vol. 6, pp. 70964–70973, 2018, doi: 10.1109/ACCESS.2018.2881277.

[24] A. Opitz, A. Falchier, G. S. Linn, M. P. Milham, and C. E. Schroeder, "Limitations of *ex vivo* measurements for *in vivo* neuroscience," *Proc. Nat. Acad. Sci. USA*, vol. 114, no. 20, pp. 5243–5246, May 2017, doi: 10.1073/pnas.1617024114.

[25] M. Akhtari, H. C. Bryant, A. N. Mamelak, E. R. Flynn, L. Heller, L. J. Shih, M. Mandelkern, A. Matlachov, D. M. Ranken, E. D. Best, M. A. DiMauro, R. R. Lee, and W. W. Sutherling, "Conductivities of three-layer live human skull," *Brain Topography*, vol. 14, no. 3, pp. 67–151, 2002, doi: 10.1023/A:1014590923185.

[26] J. Latikka, T. Kuurne, and H. Eskola, "Conductivity of living intracranial tissues," *Phys. Med. Biol.*, vol. 46, no. 6, pp. 1611–1616, 2001, doi: 10.1088/0031-9155/46/6/302.

[27] H. McCann, G. Pisano, and L. Beltrachini, "Variation in reported human head tissue electrical conductivity values," *Brain Topography*, vol. 32, no. 5, pp. 825–858, Sep. 2019, doi: 10.1007/s10548-019-00710-2.

[28] C. Gabriel, A. Peyman, and E. H. Grant, "Electrical conductivity of tissue at frequencies below 1 MHz," *Phys. Med. Biol.*, vol. 54, no. 16, pp. 4863–4878, 2009, doi: 10.1088/0031-9155/54/16/002.

[29] G. Schmid and R. Hirtl, "On the importance of body posture and skin modelling with respect to *in situ* electric field strengths in magnetic field exposure scenarios," *Phys. Med. Biol.*, vol. 61, no. 12, pp. 4412–4437, Jun. 2016, doi: 10.1088/0031-9155/61/12/4412.

[30] A. M. Dale, B. Fischl, and M. I. Sereno, "Cortical surface-based analysis: I. Segmentation and surface reconstruction," *NeuroImage*, vol. 9, no. 2, pp. 94–179, 1999, doi: 10.1006/nimg.1998.0395.

[31] B. Fischl, M. I. Sereno, R. B. Tootell, and A. M. Dale, "High-resolution intersubject averaging and a coordinate system for the cortical surface," *Hum. Brain Mapping*, vol. 8, no. 4, pp. 272–284, 1999.

[32] I. Laakso, S. Tanaka, S. Koyama, V. De Santis, and A. Hirata, "Inter-subject variability in electric fields of motor cortical tDCS," *Brain Stimulation*, vol. 8, no. 5, pp. 906–913, 2015, doi: 10.1016/j.brs.2015.05.002.

[33] W. Wang and S. R. Eisenberg, "A three-dimensional finite element method for computing magnetically induced currents in tissues," *IEEE Trans. Magn*, vol. 30, no. 6, pp. 5015–5023, Nov. 1994, doi: 10.1109/20.334289.

[34] I. Laakso and A. Hirata, "Fast multigrid-based computation of the induced electric field for transcranial magnetic stimulation," *Phys. Med. Biol.*, vol. 57, no. 23, pp. 7753–7765, 2012, doi: 10.1088/0031-9155/57/23/7753.

[35] P. C. Miranda, M. Hallett, and P. J. Basser, "The electric field induced in the brain by magnetic stimulation: A 3-d finite-element analysis of the effect of tissue heterogeneity and anisotropy," *IEEE Trans. Biomed. Eng.*, vol. 50, no. 9, pp. 1074–1085, Sep. 2003, doi: 10.1109/TBME.2003.816079.

[36] P. C. Miranda, L. Correia, R. Salvador, and P. J. Basser, "Tissue heterogeneity as a mechanism for localized neural stimulation by applied electric fields," *Phys. Med. Biol.*, vol. 52, no. 18, pp. 5603–5617, 2007, doi: 10.1088/0031-9155/52/18/009.

[37] P. C. Miranda, A. Mekonnen, R. Salvador, and P. J. Basser, "Predicting the electric field distribution in the brain for the treatment of glioblastoma," *Phys. Med. Biol.*, vol. 59, no. 15, pp. 4137–4147, Aug. 2014, doi: 10.1088/0031-9155/59/15/4137.

[38] G. B. Saturnino, A. Thielscher, K. H. Madsen, T. R. Knösche, and K. Weise, "A principled approach to conductivity uncertainty analysis in electric field calculations," *NeuroImage*, vol. 188, pp. 821–834, 2018, doi: 10.1016/j.neuroimage.2018.12.053.

[39] C. Wenger, R. Salvador, P. J. Basser, and P. C. Miranda, "The electric field distribution in the brain during TTFields therapy and its dependence on tissue dielectric properties and anatomy: A computational study," *Phys. Med. Biol.*, vol. 60, no. 18, pp. 7339–7357, Sep. 2015, doi: 10.1088/0031-9155/60/18/7339.

[40] S. B. Baumann, D. R. Wozny, S. K. Kelly, and F. M. Meno, "The electrical conductivity of human cerebrospinal fluid at body temperature," *IEEE Trans. Biomed. Eng.*, vol. 44, no. 3, pp. 220–223, Mar. 1997, doi: 10.1109/10.554770.

[41] M. Thurai, V. D. Goodridge, R. J. Sheppard, and E. H. Grant, "Variation with age of the dielectric properties of mouse brain cerebrum," *Phys. Med. Biol.*, vol. 29, no. 9, pp. 1133–1136, Sep. 1984, doi: 10.1088/0031-9155/29/9/009.

[42] C. Gabriel, "Dielectric properties of biological tissue: Variation with age," *Bioelectromagnetics*, vol. 26, no. S7, pp. S12–S18, 2005, doi: 10.1002/bem.20147.

[43] A. Peyman, A. A. Rezazadeh, and C. Gabriel, "Changes in the dielectric properties of rat tissue as a function of age at microwave frequencies," *Phys. Med. Biol.*, vol. 46, no. 6, pp. 1617–1629, 2001, doi: 10.1088/0031-9155/46/6/303.

[44] J. P. Reilly and A. Hirata, "Low-frequency electrical dosimetry: Research agenda of the IEEE international committee on electromagnetic safety," *Phys. Med. Biol.*, vol. 61, no. 12, pp. R138–R149, Jun. 2016, doi: 10.1088/0031-9155/61/12/R138.

[45] Y. Feng, R. J. Okamoto, R. Namani, G. M. Genin, and P. V. Bayly, "Measurements of mechanical anisotropy in brain tissue and implications for transversely isotropic material models of white matter," *J. Mech. Behav. Biomed. Mater.*, vol. 23, pp. 117–132, Jul. 2013, doi: 10.1016/j.jmbbm.2013.04.007.

[46] P. W. Nicholson, "Specific impedance of cerebral white matter," *Experim. Neurol.*, vol. 13, no. 4, pp. 386–401, 1965, doi: 10.1016/0014-4886(65)90126-3.

[47] J. B. Ranck and S. L. BeMent, "The specific impedance of the dorsal columns of cat: An anisotropic medium," *Experim. Neurol.*, vol. 11, no. 4, pp. 451–463, 1965, doi: 10.1016/0014-4886(65)90059-2.

[48] M. De Lucia, G. J. M. Parker, K. Embleton, J. M. Newton, and V. Walsh, "Diffusion tensor MRI-based estimation of the influence of brain tissue anisotropy on the effects of transcranial magnetic stimulation," *NeuroImage*, vol. 36, no. 4, pp. 1159–1170, Jul. 2007, doi: 10.1016/j.neuroimage.2007.03.062.

[49] Y. Diao, J. Gomez-Tames, E. A. Rashed, R. Kavet, and A. Hirata, "Spatial averaging schemes of *in situ* electric field for low-frequency magnetic field exposures," *IEEE Access*, vol. 7, pp. 184320–184331, 2019, doi: 10.1109/ACCESS.2019.2960394.

**MARCO SOLDATI** received the B.S. degree in clinical engineering and the M.S. degree in biomedical engineering from Sapienza University, Rome, Italy, in 2008 and 2011, respectively. He is currently pursuing the Ph.D. degree in electrical engineering and automation with Aalto University, Espoo, Finland.

He has several years of professional experiences in biomedical and pharmaceutical companies. His current research focused on the assessment of human exposure to low-frequency electromagnetic fields and computational modeling.

**ILKKA LAAKSO** (Member, IEEE) received the M.Sc. (Tech.) degree in electromagnetics from the Helsinki University of Technology, Espoo, Finland, in 2007, and the D.Sc. (Tech.) degree in electromagnetics from Aalto University, Espoo, in 2011.

From 2013 to 2015, he was a Research Assistant Professor and a Research Associate Professor with the Department of Computer Science and Engineering, Nagoya Institute of Technology. Since 2015, he has been an Assistant Professor in electromagnetics in health technologies with Aalto University. He has authored more than 100 papers published in international journals and conference proceedings. His current research focuses on computational bioelectromagnetic modeling for assessment of human safety and biomedical applications.

Dr. Laakso is a member of the Scientific Expert Group of the International Commission on Non-Ionizing Radiation Protection and a member of the IEEE International Committee on Electromagnetic Safety. He received several awards, including the Student Award from the International Symposium on Electromagnetic Compatibility, Kyoto, in 2009, the Ericsson Young Scientist Award in 2011, and the Young Scientist Award from the URSI General Assembly and Scientific Symposium, Montreal, Canada, in 2017.